
Heat and moisture transfer investigation of surface building materials

Carla Balocco*, Giuseppe Petrone

Department of Industrial Engineering, University of Florence, Via Santa Marta 3, Florence 50139, Italy

Corresponding Author Email: carla.balocco@unifi.it

<https://doi.org/10.18280/mmep.050303>

ABSTRACT

Received: 5 February 2018

Accepted: 9 June 2018

Keywords:

moisture buffer, adsorption/desorption, porous material, CFD, transient simulation

Numerical investigation of the capacity of porous hygroscopic building materials to damp indoor humidity variations is the aim of our present study. By means of CFD-FEM multiphysics transient simulations, taking into account relative humidity and temperature variation inside different material samples referring to the fundamental experimental test protocol on the “*Moisture Buffering of Building Materials*” (the well-known NORDTEST), all the thermo-hygrometric properties, connected to the moisture content capacity and moisture buffer effect of some building materials, were assessed. Sorption isotherm curves, that provide moisture content as a function of relative humidity, were considered. An energy balance coupled with mass transfer equation for moisture was solved considering the porous structure of the studied media. The non-isothermal method implementation allowed the investigation on the coupled relative humidity and temperature periodic variations, happened during the NORDTEST experimental application, that were used for simulate thermo-hygrometric constraints. The proposed method can be used for the efficacy evaluation of porous materials used as indoor building envelopes for passive control technique and relative humidity amplitude control.

Our research can be a useful tool for defining fundamental guidelines for any project aimed to the building-plant system energy consumption reduction and building user comfort.

1. INTRODUCTION

The opportunity of “controlling” the indoor moisture content by applying specific building materials represents a crucial item to improve thermal comfort, indoor air quality and energy saving by reducing the operating hours and/or HVAC systems downsizing.

Several ongoing academic efforts are devoted to study the suitability of using building porous hygroscopic materials to damp the indoor humidity variations due to external environmental loads and internal sources through moisture exchange. Many literature studies have demonstrated that moisture buffer capacity of hygroscopic materials can influence the indoor microclimatic conditions [1-3].

This involves thermal comfort, durability and thermo-physical performances of material/envelope, indoor air quality (IAQ) and ventilation control. It also contributes to energy saving, due to operating hours and size reduction of the heating, ventilating air conditioning (HVAC) plant system [4-7]. The use of porous materials as indoor building envelopes can be an effective passive control technique for relative humidity amplitude control.

A great deal of literature has shown the benefits from inside relative humidity variation control provided by hygroscopic materials [2-4]. Moisture buffering or damping phenomena have been investigated through the NORDTEST project on the “*Moisture Buffering of Building Materials*” started in 2003 and at the end produced an experimental test protocol [8]. Fundamentals of this protocol was the “moisture buffering” definition, that depends on sorption and vapour permeability, and an experimental method suggestion for material property

characterization usually performed inside climatic chambers by cyclical relative humidity variation (8 and 16 hrs scheme respectively at 75% and 33% at a constant air temperature of 23°C).

From an experimental point of view, several studies on this subject are based on a “material level”. That means studies are related to the international standards for moisture storage performance determination (i.e. sorption isotherms ISO 12571 [9] and vapour permeability ISO 12572 [10]) at stationary conditions for specific test section materials.

A common parameter adopted for direct assessing the experimental moisture accumulation capacity of a chosen material under transient conditions is the MBV (Moisture Buffer Value) [3]; [11-12]. Some other studies deal with a much more macroscopic approach, defined as “element/system level”. This kind of analyses mainly concern on the ideal and practical MBV and moisture effusivity offered by a “system of elements”, very often consisting in multi-layered geometries composed by variable thickness different materials [13]. This allow a “preview” of technological applications in building envelopes, in terms of measures of moisture accumulation capacity. Finally, some other experimental studies were developed by considering effective real-world conditions, adopting a so called “room level”. This approach keeps into account a whole room test section (exposure areas/volumes, moisture load, ventilation rate and indoor microclimatic conditions) in studying the moisture buffer performance of surface building materials [13]. Numerical studies were also published on this subject.

Many investigations were developed on detailed Heat, Air and Moisture (HAM) analysis of materials usually exploited

for building envelope. From a geometrical point of view, most of these studies are based on the 1-D approach, and for this reason could be restrictive to investigate on real-world applications, that can introduce variety in terms of geometrical arrangements of different materials in multi-layered building envelopes and complexity in boundary conditions definitions. Different levels of complexity of mathematical modeling on this subject were adopted [2-13].

Applied methods range from pure diffusivity models to the most complex models incorporating pore space description used to obtain the hygrothermal transport and storage functions in solving the moisture balance in each specific application. In a recent research paper, two different 3-D numerical modelling approaches, for simulation of moisture buffering in porous materials used for building applications have been provided [14]. In conjunction with experiments, numerical analyses were also developed referring to different “scaling” approach for process simulation. Usually, energy and mass balance and interface equations are implemented in simulation tools and solved using numerical methods for space and time discretization.

Basing on the present literature on this subject, the authors propose a mathematical formulation grounded in the choice of the relative humidity as driving potential and based on capillary and diffusive flux evaluation. Transient simulations were developed applying the CFD by using a finite element method (FEM) and multiphysics approach, with a non-isothermal transport-diffusion model for porous media, to a sample of building material generally used as coating for interior walls, ceiling and floor.

The insights obtained through the results can provide basilar guidelines for designing tests and simulation on moisture buffering but also selecting criteria of porous building materials with moisture damping capacity for different applications.

The proposed method can be used for analyzing, comparing and assessing the use of porous materials as indoor building envelopes such as an effective passive control technique for relative humidity amplitude control.

2. NUMERICAL MODELLING

A numerical tool for investigating the moisture buffering in building materials was built-up. Building materials are very often solid porous media in which moisture at vapour state can be transferred by diffusion and capillary suction. A characteristic curve, named as sorption isotherm, defines for each material the equilibrium moisture content in the hygroscopic and capillary water regions. This curve provides the moisture content as a function of the relative humidity: up to a relative humidity value of about 90-95% the pores of the porous solid medium are mainly filled by moisture content in the form of vapour state of matter.

Therefore, this region is known as hygroscopic region. In the hygroscopic region, the main mechanism of moisture transport is the vapour diffusion. For higher value of the relative humidity, liquid transport is possible: moisture transport is much more driven by capillary effect. In a real system, the two above mentioned mechanism co-exist, being the vapour diffusion much more active for small sized pores, while the capillary effect results preponderant for large sized ones.

2.1 Governing equations

From a mathematical point of view, the moisture balance equation can be expressed by using several thermodynamic potential as dependent variable of a transport-diffusion partial differential equation. In the present work, as well as in several literature studies [15], we adopted the relative humidity as dependent variable of the mathematical model.

This choice assures a continuous behaviour at the interface between two adjacent layers of different materials, so it is recommended in applications where moisture transfer is analysed in multi-layered shaped systems, such as the building envelopes. Under this assumption, the governing equation used for our models read as follows:

$$\xi \frac{\partial \phi}{\partial t} + \nabla \cdot \left(-\xi D_w \nabla \phi - \delta_p \nabla (\phi p_{sat}(T)) \right) = G \quad (1)$$

This equation models the moisture transfer as the sum of the vapour diffusion flux and the capillary moisture flux, being:

$$-D_w \nabla (w(\phi)) = -D_w \frac{\partial w}{\partial \phi} \nabla \phi = -\xi D_w \nabla \phi \quad (2)$$

$$\delta_p \nabla p_v(T) = \delta_p \nabla (\phi p_{sat}(T)) \quad (3)$$

In the previous equations, ϕ is the relative humidity, δ_p [$\text{m}^2 \cdot \text{s}^{-1}$] is the vapor permeability, p_{sat} is the saturation pressure [Pa], w is the moisture capacity [$\text{kg} \cdot \text{kg}^{-1}$], D_w [$\text{m} \cdot \text{s}^{-2}$] is the moisture diffusivity, G [$\text{kg} \cdot \text{m}^{-3}$] is the generic moisture source and T [K] is the temperature. The coupled thermal analysis was solved by considered the following form of the energy equation:

$$\left(\rho C_p \right)_{eff} \frac{\partial T}{\partial t} + \nabla \cdot \left(-k_{eff} \nabla T - L_v \delta_p \nabla (\phi p_{sat}(T)) \right) = Q \quad (4)$$

where ρ [$\text{kg} \cdot \text{m}^{-3}$] is the density, C_p [$\text{J} \cdot \text{kg}^{-1} \cdot \text{K}^{-1}$] is the specific heat at constant pressure, k [$\text{W} \cdot \text{m}^{-1} \cdot \text{K}^{-1}$] is the thermal conductivity, L_v [$\text{J} \cdot \text{kg}^{-1}$] the heat of evaporation, Q [$\text{W} \cdot \text{m}^{-3}$] the heat source.

The energy balance applies to the considered porous media, under assumption of local thermo-dynamical equilibrium. In the first term of equation (4), the effective thermal capacity is defined as follows:

$$\left(\rho C_p \right)_{eff} = \rho_s C_{p,s} + w C_{p,w} \quad (5)$$

The term $(\rho C_p)_{eff}$ is the effective volumetric heat capacity at constant pressure, defined to account for both solid matrix and moisture properties. In the previous equation, ρ_s is the dry solid density, $C_{p,s}$ is the dry solid specific heat capacity, w is the water content given by the moisture storage function for the chosen material, and $C_{p,w}$ is the water heat capacity at constant pressure. Similarly, k_{eff} is the effective thermal conductivity, defined in function of the solid matrix and moisture properties, as follows:

$$k_{eff} = k_s \left(1 + \frac{bw}{\rho_s} \right) \quad (6)$$

where k_s is the dry solid thermal conductivity and b (dimensionless) is a thermal conductivity supplement due to

the water content. The heat source due to moisture content variation in equation (4) is expressed as the vapour diffusion flow multiplied by latent heat of evaporation (L_v). In the same equation, the sensible heat source is otherwise labeled as Q .

Equations (1) and (4) were considered as mathematical model to numerically solve the coupled moisture and heat transfer in the medium sample.

2.2 Geometry and material

Geometry of the numerical model was chosen correspondent to an asy-to-use sample for future experimental campaign of measures. To this purpose, we considered 10 x 10 x 6 cm block, made of a material very usually employed in building applications, such as a plaster gypsum. Thermo-physical properties, porosity and hygroscopicity of material and its corresponding sorption isotherm curve were used as input data. They were taken by the material library included in the used simulation software and are given in Table 1.

Table 1. Material physical properties

Physical property	Value
Density	574[kg/m ³]
Specific heat at constant pressure	1100 [J/(kg K)]
Thermal conductivity	$k(\phi)$ [W/(m K)]
Diffusion coefficient	$D_w(\phi)$ [m ² /s]
Water content	$w(\phi)$ [kg/m ³]
Vapour resistance factor	6.9 [-]
Vapour permeability	2.9E-11[s]

Our modelling kept into account the variation with respect to the relative humidity of the water content w (moisture storage curve or sorption isotherm), the vapour diffusion coefficient D_w and the thermal conductivity k . This dependency, occurring in the space and during time, was retained during solution by exploiting the correlation curves reported in Fig. 1-3 (also held by the software material library).

2.3 Boundary conditions

Numerical solution of governing equations was carried-out by applying the boundary conditions imposed by the NORDTEST protocol [8]. We considered only two exposed faces to the controlled indoor constraints reproducing the NORDTEST [8]. In particular, practical Moisture Buffer Value (MBV) concept indicates the amount of water that is transported in or out of a material per open surface area, during a certain period of time, in the prescribed test method 8 hours of absorption [8] when the sample is subjected to cyclic variations in relative humidity of the controlled environment kept at constant temperature (23°C).

In particular, we referred to this protocol [8] for the following basic reasons: it uses 24-hour cycles that correspond to all the hours of a day so that experimental tests duration can be reduced especially for those materials such as wood would take longer time to absorb/release moisture; the cycle is divided into 8 hours of maximum air humidity value and 16 hours of minimum air humidity value to reproduce the same air humidity trend of environments with no-continuous occupancy; it defines a single value of the MBV for the hygrometric characterization of different materials allowing accurate classifications and comparisons.

On the two above explained sample faces, we applied a 24-

hours periodic smoothed time-step function for the relative humidity value, being the minimum value 33% (during 16 hours) and the maximum one 75% (during 8 hours), as prescribed in the reference protocol.

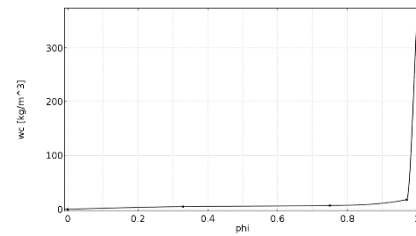


Figure 1. Material water content as a function of the relative humidity (sorption curve)

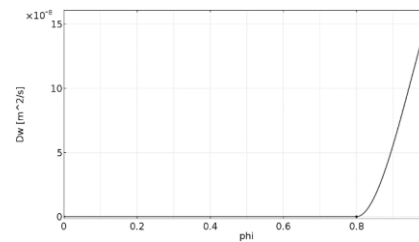


Figure 2. Material diffusion coefficient as a function of the relative humidity

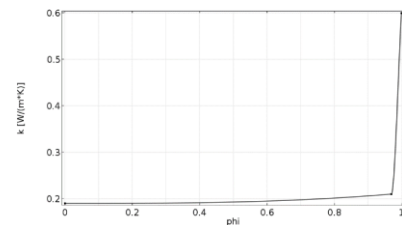


Figure 3. Material thermal conductivity as a function of the relative humidity

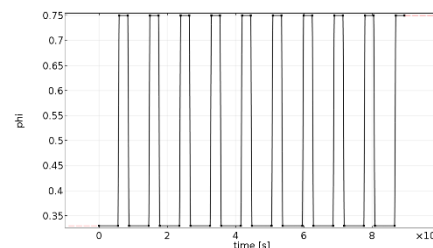


Figure 4. Material water content as a function of the relative humidity (sorption curve)

From a thermal point of view, in accordance with the NORDTEST protocol, we considered the faces exposed to a convective heat transfer exchange with an indoor fixed temperature of 23 °C. The boundary condition was applied by means of a heat flux, usually expressed as the product between a global heat exchange coefficient (h_{conv}) and the temperature difference between the wall and the environment.

This allows the evaluation of the convective surface coefficient for moisture transfer, which is usually around $2.0 \cdot 10^{-8}$ kg·m⁻²·s/Pa, and corresponds to a convective surface resistance for moisture transfer of $5.0 \cdot 10^7$ Pa/(kg·m²·s). These are normal values for environments with an ambient air velocity around 0.1 m/s [16]. All the other walls were

considered adiabatic (see Fig. 5) both for heat and moisture transport.

Insulation condition (no flux) was applied on the other (four) block surfaces (see Fig. 5) both for heat and moisture transport. The implemented boundary conditions (both in space and in time) refer to the operational thermo-hygrometric conditions defined in the NORDTEST protocol.

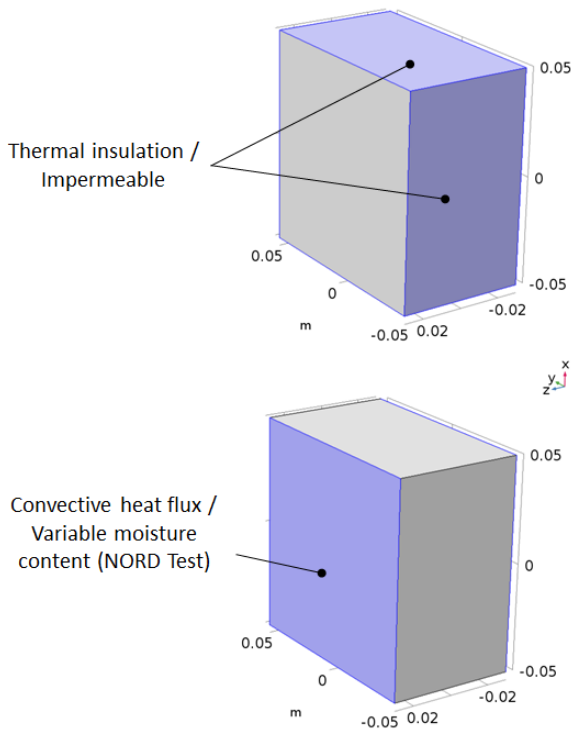


Figure 5. Graphical representation of applied boundary conditions

2.4 Numerical solution

Governing equations with their boundary conditions were numerically solved by using a FE-based approach for spatial discretization in COMSOL Multiphysics v5.2 software environment. Numerical meshes consisted of non-structured and non-uniform computational grids made up of tetrahedral Lagrange elements of the second order. The influence of spatial discretization was preliminary checked, in order to assure mesh-independent results. The MBV-practical computed by using three computational grids were compared and the relative errors with respect to the finer employed mesh result were computed. We found MBV-practical values almost constant with respect to the different meshes. Time-marching was performed by adopting an Implicit Differential-Algebraic (IDA) solver, based on a variable-order and variable-step-size Backward Differentiation Formulas (BDF). Because the time-marching scheme is implicit, a nonlinear system of equations was solved for each time step by applying a modified Newton algorithm.

Algebraic systems of equations coming from differential operator discretization were solved by a PARDISO package, a parallel direct solver particularly efficient for solving unsymmetrical sparse matrixes by a LU decomposition technique. A computational node made of a twin 64-bit quad-core CPU running at 2.3 GHz and handling 128 GB of RAM was exploited for carried-out results.

We run 10-days simulation for the considered material constituting the sample, so that 10 complete NORDTEST protocol were applied to the exposed faces of the block. We verified this number of cycles guarantees an achieved stabilization of the system response, avoiding results dependency by the initial conditions.

3. RESULTS

Moisture buffering potential of the hygroscopic materials studied was evaluated using simulation results. Thermal and moisture transfer from surrounding environment to the inner material was investigated. Figures 6-7 show time evolution of relative humidity computed at the centre of the considered block (PT_00) and in a reference point, located on the transversal axis of the block but 1 cm from one of the two exposed surfaces to the assumed thermo-hygrometric constraints (PT_01). Moisture absorption/desorption process in the tested material clearly appears.

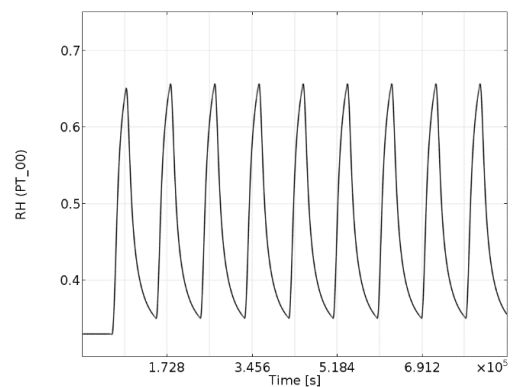


Figure 6. Time evolution of the relative humidity (RH) computed at PT_00 during 10-cycles simulation

Figures 8-9 show the computed value of the moisture content at PT_00 and PT_01 in the tested block. It can be deduced that number of simulated cycles is sufficient to avoid results influence from initial conditions.

Indeed, at the end of the second or third cycle system assumes a “permanent” periodic trend. It can be seen that the mass accumulation/loss in the studied material follows a similar pattern of moisture adsorption and desorption which in turn is strictly connected to relative humidity variation over time.

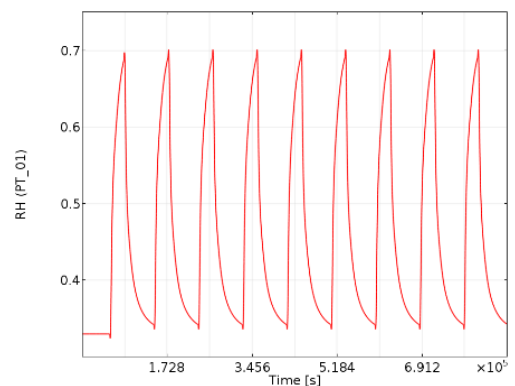


Figure 7. Time evolution of the relative humidity (RH) computed at PT_01 during 10-cycles simulation

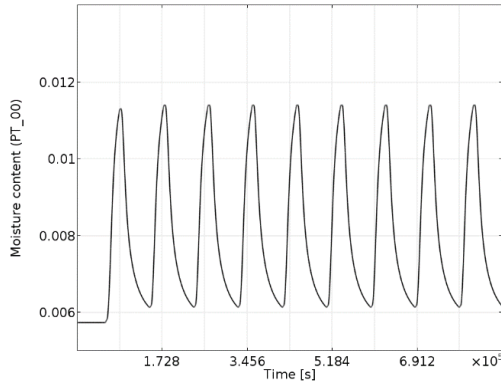


Figure 8. Time evolution of the relative humidity (RH) computed at PT_00 during 10-cycles simulation

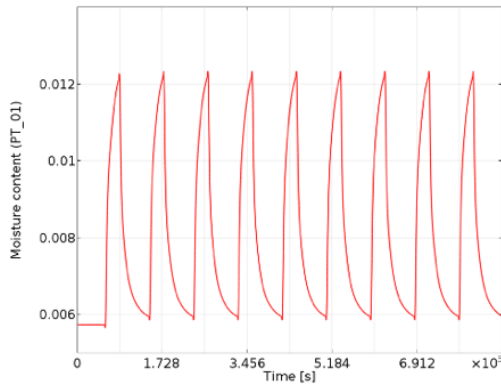


Figure 9. Time evolution of the relative humidity (RH) computed at PT_01 during 10-cycles simulation

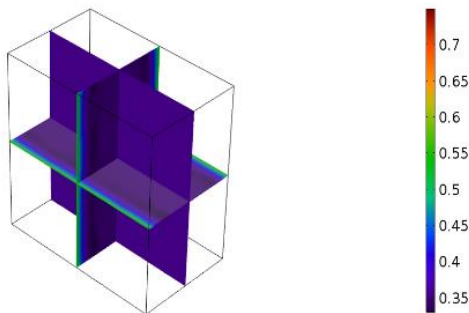


Figure 10. Multi-slice representation of relative humidity distribution after 0 hours of the 10th cycle

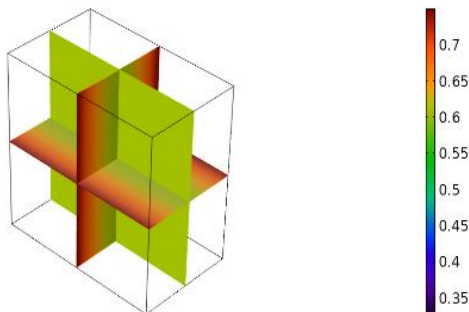


Figure 11. Multi-slice representation of relative humidity distribution after 6 hours of the 10th cycle

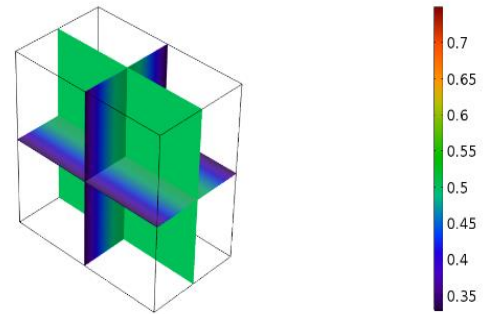


Figure 12. Multi-slice representation of relative humidity distribution after 12 hours of the 10th cycle

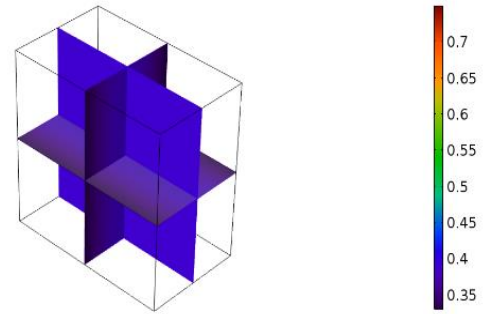


Figure 13. Multi-slice representation of relative humidity distribution after 18 hours of the 10th cycle

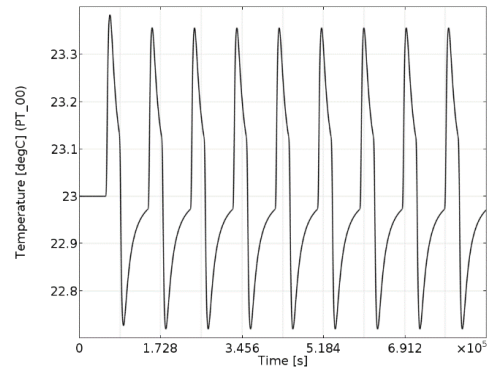


Figure 14. Time evolution of the temperature (T) computed at PT_00 during 10-cycles simulation

Figures 10-13 provide relative humidity distribution in 3 perpendicular slices of the test block, referred to different time instants of the 10th cycle applied to the test section. Moisture vapour penetration to the block and the desorption step when vapour is released to the surround environment are particularly appreciable. This result confirms that moisture buffering effect varies seasonally depending on the outdoor air conditions and indoor/outdoor ventilation.

The implementation of a non-isothermal numerical modelling allowed monitoring temperature distribution in the test section over time. Figure 14 shows temperature distribution over time, at PT_00 during the applied cycles.

Despite of the environment temperature was held at constant value, indeed 23 °C as prescribed by [8], an important temperature variation occurs inside material block. During the vapour adsorption/desorption, temperature in the block is detected to change in value over a 0.5 °C range of variation.

This provides interesting results in compliance with those of literature [2-3], [13]: temperature variations follow the absorption and desorption phases, according to surface latent heat effects. Figures 15-18 provide multi-slice representation of temperature distributions in different time instants. Graphical representations relate in particular to the 10th day of simulation and plots refer to 4 time instant (00h00, 06h00, 12h00, 18h00). Because of the transient simulation, the effect of “past” heat and mass transfer is coherently evident, such as highlighted in Figure 15 where temperature of the exposed faces to ambient is not exactly 23°C.

Analysing Figures 15-18, it can be deduced that the buffer capacity is temperature dependent, because although materials have a sorption which is very nearly unaffected by temperature, the change in water vapour concentration in space for a given RH change varies strongly with temperature. As generally demonstrated, the buffer capacity will double with a ten degree fall in temperature.

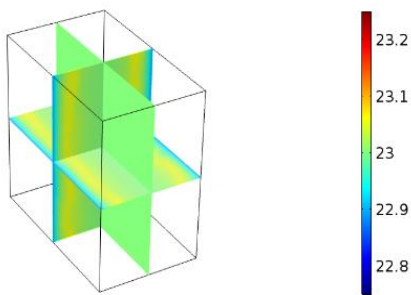


Figure 15. Multi-slice representation of temperature distribution after 0 hours of the 10th NORDTEST cycle

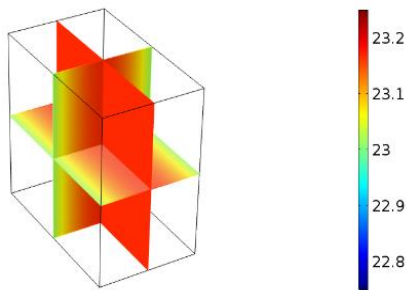


Figure 16. Multi-slice representation of temperature distribution after 6 hours of the 10th NORDTEST cycle

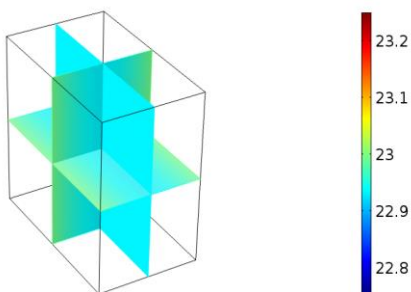


Figure 17. Multi-slice representation of temperature distribution after 12 hours of the 10th NORDTEST cycle

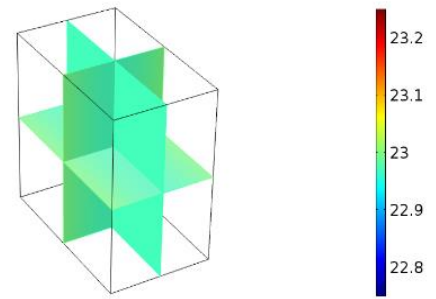


Figure 18. Multi-slice representation of temperature distribution after 18 hours of the 10th NORDTEST cycle

4. CONCLUSIONS

A numerical study was carried-out in order to simulate the moisture and heat transfer in a sample of common use surface building material. Modelling was based on a non-isothermal approach, that allows to take into account distribution and transient variation of temperature in the studied sample section during cyclic adsorption and desorption processes.

The sorption curve was used to relate the moisture content with the relative humidity.

This last mentioned potential was chosen as dependent variable for numerical simulation of the vapour transfer.

In order to execute a first run of our models, the well-known NORDTEST was retained as thermal and hygroscopic constraints for simulations. Time-dependent computations were carried-out for a period of 10 cycles. Duration was long enough to avoid dependency of results from initial conditions. Results were post-processed in order to monitoring punctual time-evolution of the dependent variables, but also by means of spatial distribution at a chosen time instant. From results, the adsorption/desorption mechanism clearly appears. The non-isothermal approach exploited in simulation allowed to monitoring temperature variation inside the test section despite of a constant temperature hold in the surrounding environment. This provides the knowledge of an interesting aspect to pursue and validate against future experimental measurements.

In addition, obtained results, that are useful for describing the moisture content variation in materials at slight depths from the exposed boundary (both indoor and outdoor), show the preponderant role of vapour permeability and porosity of materials for the moisture capacity and moisture damping effects. Our research can be a useful tool for the using of porous materials as indoor building envelopes as an effective passive control technique of relative humidity amplitude.

REFERENCES

- [1] Di Giuseppe E, D’Orazio M. (2014). Moisture buffering active devices for indoor humidity control: preliminary experimental evaluations. *Energy Procedia* 64: 42-51. <http://dx.doi.org/10.1016/j.egypro.2014.12.365>
- [2] Ge H, Yang X, Fazio P, Rao J.(2014). Influence of moisture load profiles on moisture buffering potential and moisture residuals of three groups of hygroscopic materials. *Building and Environment* 81: 162-171. <http://doi.org/10.1016/j.buildenv.2014.06.021>

- [3] Rode C, Hens H, Janssen H. (2008). IEA Annex 41 whole building heat, air, moisture response. Proc. of Closing Sem., Nordic Building Physics Conf. Danish Society of Engineers, IDA. (BYG Rapport; No. R-189).
- [4] Salonvaara M, Ojanen T, Holm A, Künzel HM, Karagiozis AK. (2004). Moisture buffering effects on indoor air quality. Experimental and Simulation Results. ASHRAE Rep.
- [5] Baofei C. (2017). Study on building energy consumption performance of composite polystyrene granule thermal insulation mortar. Chemical Engineering Transactions 62: 319-324. <http://doi.org/10.3303/CET1762054>
- [6] Zuo G, Jia S, Gao H. (2016). The influence of the traditional architecture patio with cover on the ventilation of the indoor air pressure. Chemical Engineering Transactions 51: 187-192. <http://doi.org/10.3303/CET1651032>
- [7] Yang WG, Hub XY, Wua SY, Cheng ZG. (2018). Analysis of thermal defects on exterior wall insulation system. Chemical Engineering Transactions 66: 325-330. <http://doi.org/10.3303/CET1866055>
- [8] Rode C, Peuhkuri RAD. (2006). moisture buffering of building materials. NORDTEST, Report BYG DTU R-126.
- [9] ISO 12571 (2013). Hygrothermal performance of building materials and products. Determination of hygroscopic sorption properties.
- [10] ISO 12572 (2016). Hygrothermal performance of building materials and products. Determination of water vapour transmission properties. Cup method.
- [11] Woods J, Winkler J, Christensen D. (2013). Evaluation of the effective moisture penetration depth model for estimating moisture buffering in buildings. NREV, Tech. Rep. NREL/TP-5500-57441.
- [12] Maliki M, Laredj N, Naji H, Bendani K, Missoum H. (2012). Numerical modelling of hygrothermal response in building envelopes. GRAĐEVINAR Report 66, 11: 987-995.
- [13] Nuno MM, Ramos NMM, De Freitas VP. (2012). The evaluation of hygroscopic inertia and its importance to the hygrothermal performance of buildings. Heat and Mass Transfer in Porous Media, Advanced Structured Materials 13: 24-45. http://doi.org/10.1007/978-3-642-21966-5_2
- [14] Balocco C, Petrone G. (2016). efficiency of different basic modelling approaches to simulate moisture buffering in building materials. The Open Construction & Building Technology Journal 10: 561-574. <http://doi.org/10.2174/1874836801610010561>
- [15] Tariku F, Kumaran K, Fazio P. (2010). Integrated analysis of whole building heat, air and moisture transfer. Int. J. of Heat and Mass Transfer 53: 3111-3120. <http://doi.org/10.1016/j.ijheatmasstransfer.2010.03.016>.
- [16] Rode C, Peuhkuri R, Svennberg K, Ojanen T, Mukhopadhyaya P, Kumaran M, Dean W, Moisture S. (2007). Buffer value of building materials. Journal of ASTM International 4(5). <http://doi.org/doi.org/10.1520/JAI100369>

NOMENCLATURE

C_p	Specific heat, J. kg ⁻¹ . K ⁻¹
D_w	Moisture diffusivity, m.s ⁻²
G	Moisture source, kg.m ⁻³
k	Thermal conductivity, W.m ⁻¹ . K ⁻¹
L_w	Latent heat, J.kg ⁻¹
p_{sat}	Saturation pressure. Pa
Q	Heat source, W.m ⁻³
T	Temperature, K
t	Time, s
w	Water content, kg.kg ⁻¹

Greek symbols

δ_p	Vapour permeability, m ² . s ⁻¹
ϕ	Relative humidity
ρ	Density, kg.m ⁻³
ξ	Moisture content, kg.m ⁻³